Research Article

Basharat Ullah, Umair Afzal, Asif Waheed, Umar Khan*, Walid Emam, and Hamiden Abd El-Wahed Khalifa

Significance of nanoparticle aggregation for thermal transport over magnetized sensor surface

https://doi.org/10.1515/ntrev-2024-0089 received March 16, 2024; accepted July 31, 2024

Abstract: This article explores the dynamics of nanofluids consisting of copper (TiO2) nanoparticles suspended in water, as they interact with sensor surfaces between two parallel squeezing plates with porous characteristics. This research specifically targets applications involving enhanced heat transfer and magnetohydrodynamic (MHD) control in nanofluid systems. The primary aim is to analyze the effects of nanoparticle aggregation and non-aggregation on sensor surfaces, considering MHD formations and heat transfer in the energy and momentum equations. The research adopts a steady-state fluid condition and utilizes similarity transformations to convert partial differential equations into more manageable ordinary differential equations. The methodology involves shooting methods for solving these nonlinear ordinary differential equations and employs graphical analyses to study the impacts of various parameters such as permeability, magnetic influence, squeeze flow, and radiation on the temperature and velocity profiles of the nanofluid. The results reveal significant dependencies of temperature and velocity profiles on the studied parameters, illustrating varied behaviors in scenarios of both aggregation and non-aggregation of nanoparticles. The findings emphasize how each parameter distinctively influences the heat and flow characteristics of the nanofluid, offering insights into optimizing conditions for better performance and control in practical applications. Future research could focus on extending the model to include transient fluid states and exploring the effects of other nanoparticle materials and shapes. There is also potential to investigate the interactions under different environmental conditions and to incorporate more complex boundary conditions to simulate real-world applications more accurately. Further experimental validation of the theoretical predictions would be beneficial to enhance the reliability and applicability of the findings.

Keywords: sensor surface, aggregation nanoparticle, thermal radiation, magnetic parameter, numerical investigation

Nomenclature

а

squeeze flow strength

* Coverage of Mathematics
* Corresponding author: Umar Khan, Department of Mathematics
and Statistics, Hazara University, Mansehra 21120, Pakistan,
e-mail: umar_jadoon4@yahoo.com
Basharat Ullah: College of Aerospace and Civil Engineering, Harbin
Engineering University, Harbin 150001, P R China; Department of
Mathematics, Mohi-ud-Din Islamic University, Nerian Sharif, Azad Jammu

Umair Afzal: Department of Mathematics and Statistics, Hazara University, Mansehra 21120, Pakistan

and Kashmir, Pakistan

Asif Waheed: Department of Mathematics, COMSATS University Islamabad, Attock Campus, Attock, Pakistan

Walid Emam: Department of Statistics and Operations Research, Faculty of Science, King Saud University, P. O. Box 2455, Riyadh 11451, Saudi Arabia

Hamiden Abd El-Wahed Khalifa: Department of Operations and Management Research, Faculty of Graduate Studies for Statistical Research, Cairo University, Giza 12613, Egypt

squeeze flow index b В magnetic field (T) D fractal index k* absorption coefficient (1/m) $K_{\rm f}$ thermal conductivity of the base fluid (W/m K) thermal conductivity of the nanofluid (W/m K) $K_{\rm nf}$ thermal conductivity of the nanoparticles (W/m K) M magnetic field parameter radii of aggregates and nanoparticles (m) $r_{\rm a}, r_{\rm p}$ Prandtl number Pr pressure (Pa) p radiative heat flux in the y-direction (W/m²) $q_{\rm r}$ R radiation parameter s constant S permeability parameter T temperature of nanofluid (K)

temperature of the nanofluid far away from the

 T_{∞}

surface (K)

2 — Basharat Ullah et al. DE GRUYTER

t	time (s)
U	free stream velocity (m/s)
u, v	velocity components in the <i>x</i> - and <i>y</i> -direction,
	respectively (m/s)
ν	kinematic viscosity of the fluid (m²/s)
$\mu_{ m f}$	dynamic viscosity of the base fluid (Pas)
$\mu_{ m nf}$	effective dynamic viscosity of nanofluid (Pas)
$ ho_{ m f}$	density of a base fluid (kg/m³)
$ ho_{ m nf}$	effective density of the nanofluid (kg/m³)
$ ho_{ m s}$	density of the nanoparticles (kg/m³)
$(\rho C_{\rm p})_{\rm nf}$	heat capacitance of the fluid (J/m³ K)
$(\rho C_{\rm p})_{\rm s}$	heat capacitance of the nanoparticles (J/m³ K)
$(\rho C_p)_{\mathrm{f}}$	heat capacitance of the base fluid (J/m³ K)
$\sigma_{ m f}$	electric conductivity of a base fluid (S/m)
$\sigma_{ m nf}$	electric conductivity of nanofluid (S/m)
$\sigma_{\!\scriptscriptstyle m S}$	electric conductivity of nanoparticles (S/m)
$\phi_{ m a}$	volume fraction of nanoparticle aggregates
$\phi_{ m m}$	maximum volume fraction of nanoparticles
η	similarity variable
θ	dimensionless temperature
σ^*	Stefan Boltzmann constant (W/m² K⁴)
ϕ	nanoparticle volume fraction

1 Introduction

Engineers and scientists have experimented with a wide range of methods to limit temperature increases during mechanical and industrial processes. Scientists have worked to enhance the thermal characteristics of materials because of their importance in our daily lives. They play an important role in our daily lives. The amount of heat transfer is dependent on the thermal conductivity. To improve the heat transfer efficiency, scientists conduct experiments using a variety of fluids. The inefficiency of heat transfer is a direct result of the low thermal conductivity and poor conduction of common fluids. Common fluids with low thermal conductivity ratings, such as water, kerosene oil, and ethylene glycol, cause the system temperature to rise. This issue has been addressed by the creation of nanofluids. Alumina, copper, gold, and silver nanofluids were proposed by scientists as a means of improving the thermal conductivity of these fluids.

Nanofluid was initially described by Choi and Eastman [1]. When the primary fluid is combined with nanoparticles, each of which possesses unique physical and chemical characteristics, the resulting substance is called a nanofluid. Compared to the primary fluid, its thermal conductivity is higher. There are several applications for nanoparticles in modern society. This cutting-edge innovation enhances

fluids' thermal efficiency. In the West, it is utilized for culinary, textile, and cosmetic purposes in addition to military training. Heat transmission can be enhanced by using nanofluids, which have many applications in engineering and industry. The efficiency of heat transfer in fluids with low thermal conductivity is improved by the addition of nanoscale solid particles. In recent years, nanofluid has emerged as an integral aspect of the energy transfer phenomenon. The improved heat transfer qualities of the system are useful in several contexts, including solar synthesis, gas sensing, biological sensing, nuclear chemical reactors, and the chemical industries.

It was proposed to increase the efficiency of heat transmission in common fluids by strategically placing nanoparticles in similar areas. In contrast, the researchers found that combining two or more nanoparticles into the base fluid resulted in enhanced thermal properties of the nanofluid, leading to the term "hybrid nanofluid." This type of nanofluid consists of two or more nanoparticles of different types (metallic or non-metallic) mixed with a base fluid. When compared to a pure or conventional nanofluid, the thermal conductivity and heat transfer efficiency of a hybrid nanofluid are significantly higher. This study demonstrates the effects of coating a sensor surface with nanoparticles. The growing industrial applications and significance of nanoparticles in numerous engineering processes make a comprehensive analysis of nanoparticle aggregation essential. However, the correct deformation of a plastic sheet is not always linear. The technical significance of flow and heat transport properties past a progressively stretched layer is enhanced. Using thermos physical property models, we test the interaction of a base polymer with copper oxide and titanium dioxide and water with alumina to learn more about the aggregation component of the nanoparticles.

Squeeze flow describes the motion of a substance between two parallel plates or objects, where it is compressed or twisted. An expanding droplet, its temperature, the area of contact with the plate surfaces, and the effects of both internal and external factors are all shown. Squeeze flow is used in many scientific and engineering fields, including rheology, welding engineering, and materials science. There are several applications in industry, chemistry, and biology for squeezed flow with heat transfer across a sensor surface. One category of these surfaces is sensor surfaces. Medical, biological, and chemical engineering all rely heavily on the research of thermal transport in and over sensor surfaces. Therefore, this research is conducted to evaluate heat transmission in light of the most important factors. One type of such surface is a sensor surface. The sensing elements of many biological and chemical sensors are extending surfaces.

In addition, models of thermal conductivity were presented by Koo and Kleinstreuer [2]. Many industrial processes necessitate the development of energy-efficient heat transfer fluids, but these fluids present unique challenges due to their low thermal conductivity.

Using metallic nanoparticles suspended in traditional heat transfer fluids, we propose here a new class of heat transfer media. The generated nanofluids have the highest chance of increasing heat transfer efficiency due to their predicted higher thermal conductivities compared to conventional heat transfer fluids. Khaled and Vafai [3] introduced a novel idea by studying the flow over a sensor surface in a narrow channel subject to magnetohydrodynamics (MHD) effects. They discovered that as the squeezing free stream velocity increased, the local Nusselt number and local wall shear stress also increased. Since then, scientists have investigated the issue of fluid movement across a sensor surface. It is important, and it can uncover hazardous compounds or diagnose a variety of disorders. This has made the study of heat transfer via a sensor plate of particular interest to academics and professionals.

In recent years, the nanofluid industry as a whole has become increasingly important, and shipping is no exception. Modern industrial and thermal processes rely heavily on physical properties such as heat capacity and thermal conductivity. Heat conduction to working fluids such as ethylene glycol, silicone oil, and water has been impeded by the material's poor thermal behavior. Researchers have been hard at work developing novel nanoparticles for improved thermal and cooling systems because of the significant industrial impact of fluid thermal efficiency. Due to their widespread use in cooling systems, alumina nanofluids have piqued the interest of the scientific community. The idea of Khaled and Vafai is adapted for turbulent squeezing flow by Siddiqui et al. [4]. In an experiment utilizing water as the basic fluid, Madhu et al. [5] investigated the cooling application.

Sheikholeslami and Vajravelu [6] investigated the impact of an asymmetric magnetic field on the motion of nanofluids subjected to bottom-up heating. According to the work of Manjunatha et al. [7], nanofluids are theoretically guaranteed to be more stable on solid surfaces and to have superior drenching, spreading, and widely distributed properties. Abrar [8] explored how nanoparticles of titanium dioxide moved heat around while suspended in various dilute solutions. They discovered that as the squeezing free stream velocity increased, the local Nusselt number and local wall shear stress also increased. Since then, scientists have investigated the issue of fluid movement across a sensor surface. Nadeem et al. [9] analyzed the flow and thermal properties of hybrid nanofluids over curved surfaces,

highlighting the importance of surface curvature. Nanofluid flow through a sensor surface has also been investigated in different ways by many authors [10-15]. Li et al. [16] used a titanic nanoliquid that was based on ethylene glycol in order to explore the effect that nanoparticle aggregation has on heat transmission in a Maranon convective flow. They went into great depth on the process by which nanoparticles cluster together. Significant changes were made to the thermal's physical features. After much investigation, it was found that nanoparticles do in fact exist. As the process of aggregation continued, the viscosity became more intense. Heat transfer of nanofluid through a wedge was studied by Ellahi et al. [17] observed the nanoparticle as clusters linked together. In order to study the transverse MHD flow of Al₂O₃-Cu/H₂O nanofluid under the action of active radiation, this study introduces a novel hybrid model. The results corroborate the claim made by Gangadhar et al. [18] that radiative and magnetic influences significantly influence the improvement of thermal transport specs.

Khaled and Vafai [19] demonstrate that a magnetic field applied to thin films can mitigate flow instabilities brought on by strong squeezing effects. However, studies on how a magnetic field influences flow, and thus how much heat and mass transfer occurs across a sensor surface located inside fluidic cells under compressed flow circumstances, are scarce in the literature. The influence of nanoparticle aggregation on the radiative properties of nanofluids was studied by Chen et al. [20]. The research that was carried out by Reddy et al. [21] was detailed in its investigation of the factors that led to aggregation and how it impacted the overall performance of nanofluids. The purpose of this study is to offer a comprehensive overview of the literature concerning the impact that nanoparticles have on the laminar heat transfer of nanofluids. Hussein et al. [22] give a comprehensive assessment of the existing literature as well as future directions in the subject. They examine a wide range of characteristics that have an effect on the performance of heat transfer, including particle size, concentration, and aggregation. Therefore, this research is conducted to evaluate heat transmission in light of the most important factors. It is being investigated by Krishna et al. [23] how a porous sensor surface affects the flow of a squeezed hybrid nanofluid. Sarkar et al. [24] found that nanoparticle aggregation stabilizes nanofluids and improves heat transfer performance. Compressed hybrid nanofluids pass via a porous sensor. Researchers have likely employed various nanofluid models to depict the flow through sensor surfaces. Despite this, their effectiveness is limited to providing basic descriptions. This study employs aggregation nanofluid models to explore the flow and heat transmission of nanofluids on a sensor surface. Our research aims to contribute to

the current body of knowledge by filling in specific knowledge gaps. We consider the flow, heat transfer, and MHDs of nanofluid across sensor surfaces in the context of copper (TiO₂) with water serving as the base fluid. This applies to both steady and unsteady squeezed flows in two dimensions. We devise numerical solutions to solve nonlinear ordinary differential equations. We have supplied the effects of several parameters that influence the momentum and energy equations in the form of a graphical representation. These parameters include permeability, magnet city, squeezing flow index, and radiation properties.

2 Formulation of governing equations

The influence of flow, heat transfer, and MHDs of nanofluid across sensor surfaces are addressed for a two-dimensional unsteady squeezed flow of titanium dioxide (TiO₂) in water as the base fluid. We choose the Cartesian axes to be x and y, with x running parallel to the sensor surface and y running perpendicular to it. We suppose that the lower plate remains stationary while the upper plate is subjected to squeezing action, with the free stream beginning at the surface's tip. The free stream velocity of the sensor surface U(x,t)=ax, and the temperature sensor surface is $T=T_{\infty}+\left(\frac{q_0x}{k_f}\right)\left(\sqrt{\frac{v_f}{a}}\right)\theta(\eta)$, where a is the strength of the squeeze flow and T_{∞} is the ambient temperature and is a constant. The track's height h(t) creates a narrow passageway in which the sensor surface (L) is located. The shape of the boundary layer flow is shown in Figure 1.

The following are the governing equations of motion based on the aforesaid hypothesis.

3 Governing equations

See Khaled and Vafai [3] and Rehman et al. [25] for the governing equations:

$$\frac{\partial u}{\partial x} + \frac{\partial v}{\partial y} = 0, (1)$$

$$\frac{\partial u}{\partial t} + u \frac{\partial u}{\partial x} + v \frac{\partial u}{\partial y} = \frac{\partial U}{\partial t} + U \frac{\partial U}{\partial x} + \frac{\mu_{\rm nf}}{\rho_{\rm nf}} \frac{\partial^2 u}{\partial y^2} + \frac{\sigma_{\rm nf}}{\rho_{\rm nf}} B^2 (U - u),$$
(2)

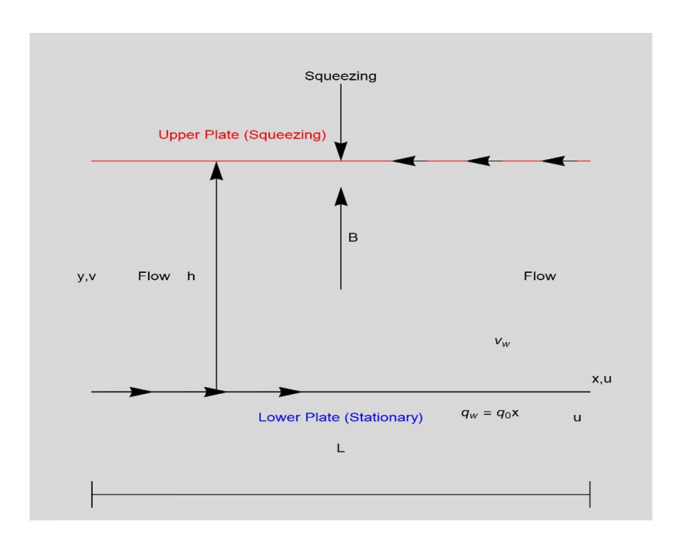


Figure 1: Geometry of the problem.

$$\frac{\partial T}{\partial t} + u \frac{\partial T}{\partial x} + v \frac{\partial T}{\partial y} = \frac{1}{(\rho C_{\rm p})_{\rm nf}} \left[\left(k_{\rm nf} + \frac{16\sigma^*}{3k^*} T^3 \right) \left(\frac{\partial^2 T}{\partial y^2} \right) \right].$$
(3)

The x- and y-components of the velocity, u and v, respectively, T is the temperature, p is the pressure, U is the free stream velocity, qr is the radiative heat flux, U, k^* is the absorption coefficient, and σ^* is the Stefan–Boltzmann constant.

Constants for dynamic viscosity ($\mu_{\rm nf}$), effective density ($\rho_{\rm nf}$), electrical conductivity, thermal conductivity, and heat capacitance are ($\sigma_{\rm nf}$), ($k_{\rm nf}$), and (($\rho C_{\rm p}$) $_{\rm nf}$), respectively.

Nanoparticles are selected for their thermophysical qualities based on their aggregation property. The effective viscosity and thermal conductivity without aggregation are calculated using Brinkman and Maxwell's models. Table 1 represents the thermophysical models.

The dynamic viscosity of the base fluid is denoted by the symbol (μ_f) . The density of the base fluid is given by (ρ_f) , the density of the nanoparticles is (ρ_s) , the electrical conductivity of the nanoparticles is (σ_{nf}) , while the electrical conductivity of the base fluid is (σ_f) , and the thermal conductivity of the nanoparticles is denoted by the symbol (k_f) . The nanoparticle volume fraction is denoted by (ϕ) . The volume fraction as a function of the most significant packing fraction in the aggregate is given by ϕ_a , whereas the volume fraction as a function of the aggregate as a

whole is indicated by $\phi_{\rm a}=\phi\left(\frac{r_{\rm a}}{r_{\rm p}}\right)^{3-D}$. Assuming the aggregates are spherical and that diffusion is the limiting factor in the aggregation process.

$$D = 1.8, \frac{r_a}{r_b} \phi_m = 3.34, \phi_m = 0.605 \text{ and } [\eta] = 2.5.$$

The overall thermal conductivity (k_a) was determined using the following steps:

Table 1: Effective thermo physical models for nanoliquids

Effective properties	Without aggregation	With aggregation
Density	$\frac{\rho_{\rm nf}}{\rho_{\rm f}}$ = $(1-\phi)$ + $\frac{\partial_{\rm s}}{\rho_{\rm f}}$	$\frac{\rho_{\rm nf}}{\rho_{\rm f}} = (1 - \phi_{\rm a}) + \phi_{\rm a} \frac{\partial_{\rm s}}{\rho_{\rm f}}$
Dynamic viscosity	$\frac{\mu_{\rm nf}}{\mu_{\rm f}} = \frac{1}{(1-\phi)^{2.5}}$	$\frac{\mu_{\rm nf}}{\mu_{\rm f}} = \left(1 - \frac{\phi_{\rm a}}{\phi_{\rm m}}\right)^{[\eta]\phi_{\rm m}}$
Electrical conductivity	$\frac{\sigma_{\rm nf}}{\sigma_{\rm f}} = \frac{\sigma_{\rm S} - 2\sigma_{\rm f} - 2\phi(\sigma_{\rm f} - \sigma_{\rm S})}{\sigma_{\rm S} - 2\sigma_{\rm f} + \phi(\sigma_{\rm f} - \sigma_{\rm S})}$	$\frac{\sigma_{\rm nf}}{\sigma_{\rm f}} = \frac{\sigma_{\rm S} - 2\sigma_{\rm f} - 2\phi(\sigma_{\rm f} - \sigma_{\rm S})}{\sigma_{\rm S} - 2\sigma_{\rm f} + \phi(\sigma_{\rm f} - \sigma_{\rm S})}$
Specific heat capacity	$\frac{(\rho C_p)_{\rm nf}}{(\rho C_{\rm p})_{\rm f}} = (1 - \phi) + \phi \frac{(\rho C_{\rm p})_{\rm s}}{(\rho C_{\rm p})_{\rm f}}$	$\frac{(\rho C_{\rm p})_{\rm nf}}{(\rho C_{\rm p})_{\rm f}} = (1 - \phi_{\rm a}) + \phi_{\rm a} \frac{(\rho C_{\rm p})_{\rm s}}{(\rho C_{\rm p})_{\rm f}}$
Thermal conductivity	$\frac{k_{\rm nf}}{k_{\rm f}} = \frac{(k_{\rm S} - 2k_{\rm f}) - 2\phi(k_{\rm f} - k_{\rm S})}{(k_{\rm S} - 2k_{\rm f}) - \phi(k_{\rm f} - k_{\rm S})}$	$\frac{k_{\rm nf}}{k_{\rm f}} = \frac{(k_{\rm a}-2k_{\rm f})-2\phi_{\rm a}(k_{\rm f}-k_{\rm a})}{(k_{\rm a}-2k_{\rm f})-\phi_{\rm a}(k_{\rm f}-k_{\rm a})}$

$$\frac{k_{\rm a}}{k_{\rm f}} = \frac{1}{4} \left[(3\varnothing_{\rm in} - 1) \frac{k_{\rm s}}{k_{\rm f}} + (3(1 - \varnothing_{\rm in}) - 1) + \left[\left[(3\varnothing_{\rm in} - 1) \frac{k_{\rm s}}{k_{\rm f}} + (3(1 - \varnothing_{\rm in}) - 1) \right]^2 + 8 \frac{k_{\rm s}}{k_{\rm f}} \right]^{\frac{1}{2}} \right].$$
(4)

Here,
$$\varnothing_{\text{in}} = \left(\frac{r_a}{r_p}\right)^{D-3}$$
.

The following are the boundary conditions:

$$u(x, 0, t) = 0, \ v(x, 0, t) = v_t,$$

 $q_w(x) = -k_{nf} \frac{\partial T(x, 0, t)}{\partial v},$ (5)

$$u(x, \theta, t) = U(x, t), T(x, \infty, t) = T_{\infty}, \tag{6}$$

where T is the surface temperature of the sensor, U(x,t) is the velocity of the free stream, and T_{∞} is the temperature of the free stream. Partial differential equations are just as difficult to solve as nonlinear equations. Using transformations of similarity, we normalize a partial differential equation. The following are some of how these variants are similar.

$$\eta = \sqrt{\frac{a}{v_f}}y, \ u = axf'(\eta), \ a = \frac{1}{(s+bt)},$$

$$v = -\sqrt{av_f}f(\eta), \text{ and } \theta(\eta) = \frac{T - T_\infty}{(q_0x/k_f)\sqrt{v_f/a}},$$

$$U(x,t) = ax.$$
(7)

Transforming equations (1)–(3).

$$\frac{\mu_{\rm nf}/\mu_{\rm f}}{\rho_{\rm nf}/\rho_{\rm f}}f'''(\eta) + \left[f(\eta) - \frac{b\eta}{2}\right]f''(\eta) - (f'(\eta))^{2} + b(f'-1) \\
+ \frac{\sigma_{\rm nf}/\sigma_{\rm f}}{\rho_{\rm nf}/\rho_{\rm f}}M(1-f') + 1 = 0.$$
(8)

$$M = \frac{v_{\rm f}}{v_{\rm o}} \sigma_{\rm f} B^2,$$

where M is the magnetic parameter.

$$\frac{1}{\Pr} \frac{1}{\frac{(\rho C_{p})_{nf}}{(\rho C_{p})_{f}}} \left(\frac{k_{nf}}{k_{f}} + \frac{4}{3}R \right) \theta''(\eta) + \left(f(\eta) + \frac{b\eta}{2} \right) \theta'(\eta)
- \left(f'(\eta) + \frac{b}{2} \right) \theta(\eta) = 0,$$

$$R = \frac{4\sigma^{*}T^{3}}{k_{f}k^{*}}, \Pr = \frac{(\rho C_{p})_{f}}{k_{f}},$$
(9)

where R is the parameter of radiation and Pr represents the Prandtl number.

In the simplified form, the boundary conditions are

$$f(0) = -S, f'(0) = 0, f'(\infty) = 1,$$
 (10)

$$\theta(\infty) = 0, \ \theta'(0) = -\frac{k_{\rm f}}{k_{\rm nf}}.$$
 (11)

4 Solution procedure

The regulation that governs the flow *via* the sensor surface is described mathematically through equations. Mathematical expressions (8)–(11) are used to explain the motion of a nanofluid, and they are solved by means of a numerical method. The underlying equation is converted into an initial value issue by firing it. We devised a rescue strategy to accomplish this. After that, the right solution is applied, which in this case is a coding scheme, and the problem is fixed. Mathematica, a mathematical computer language, is used for all graphical analysis and simulations. The steps outlined below help accomplish the goal.

$$y_1 = f(\eta),$$

 $y_2 = f'(\eta),$
 $y_3 = f''(\eta),$
 $y_4 = f'''(\eta),$
 $y_5 = \theta(\eta),$
 $y_6 = \theta'(\eta),$
 $y_7 = \theta''(\eta).$

These calculations, along with the average velocity and temperatures, provide us with the data we need.

$$\frac{\mu_{\rm nf}/\mu_{\rm f}}{\rho_{\rm nf}/\rho_{\rm f}} y_4 + \left[y_1 - \frac{b\eta}{2} \right] y_3 - (y_2)^2 + b(y_2 - 1)
+ \frac{\sigma_{\rm nf}/\sigma_{\rm f}}{\rho_{\rm nf}/\rho_{\rm f}} M(1 - y_2) + 1 = 0,$$
(12)

$$\frac{1}{\Pr} \frac{1}{\frac{(\rho C_p)_{nf}}{(\rho C_p)_f}} \left(\frac{k_{nf}}{k_f} + \frac{4}{3} R \right) y_7 + \left(f(\eta) + \frac{b\eta}{2} \right) y_6$$

$$- \left(f'(\eta) + \frac{b}{2} \right) y_5 = 0.$$
(13)

5 Results and discussions

In this section, we look at how the flow and heat transmission of nanofluids over a sensor surface are affected by their aggregation or lack thereof. Heat transport qualities over a sensor surface in a magnetic field and radiation environment are measured using nanofluid. The numerical solution is found by adjusting the values of M, R, S, and b. Properly understanding velocity and temperature curves requires investigating the effects of dimensionless parameters.

5.1 Interpretation of results

In this section, we look at how different parameters affect the resulting velocity and temperature profiles. Thermophysical properties of nanofluids are shown for a range of parameter values in Table 2. Images are provided that can be used to interpret a range of dimensionless parameter variations.

5.2 Velocity profile for TiO₂-H₂O

This section examines the turning factor distribution velocity. The graphs allow us to assess how well a flow performs given a range of input characteristics. Therefore, increasing the value of ϕ results in an increase in velocity distribution both with and without aggregation. Nevertheless, increasing the velocity with accumulation is more beneficial than values without assembly, as shown in Figure 2. As M increases, the velocity distribution expands for both cases. However, the increase in velocity with the collection is more significant than the values for points without aggregation shown in Figure 3. The velocity distribution grows for both with and without accumulation as S is decreased. However,

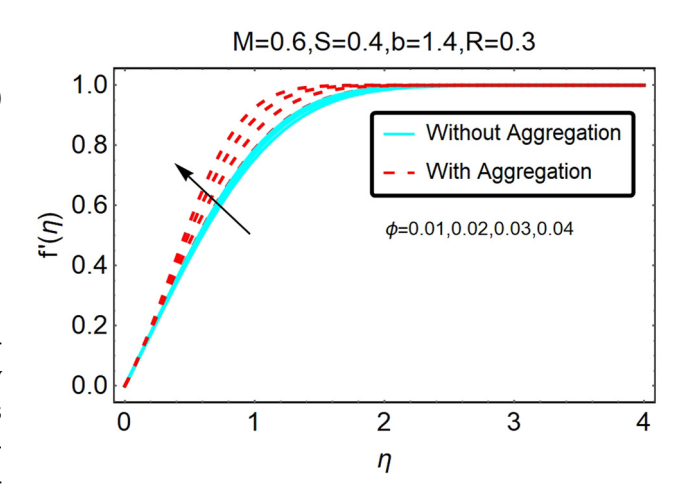


Figure 2: Velocity variation profile with changes in ϕ .

the increase in velocity with the collection is more effective than values without aggregation given in the figure.

A change in the value results in a difference in the speed profile, as shown in Figure 2. As the value of ϕ rises, the speed profile tends to grow as well. A velocity increase with aggregation is more effective than an increase without aggregation.

Figure 3 shows the evolution of the velocity profile as the value of M changes. The velocity profile typically tends to increase along with the value of M. Conversely, velocity increases with aggregation are more effective than velocity increases.

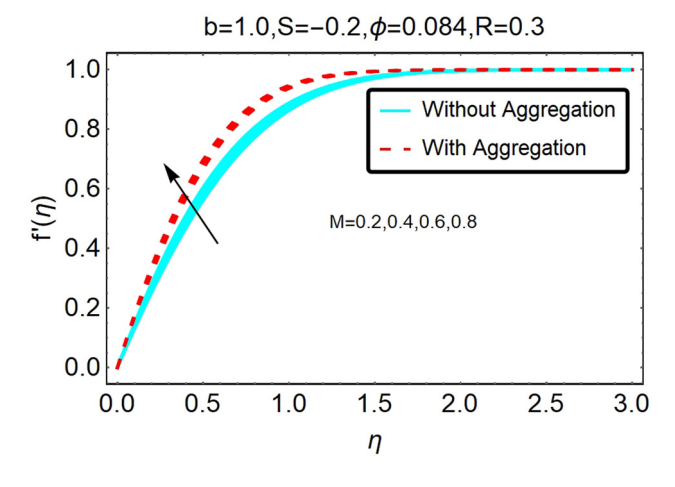


Figure 3: Velocity variation profile with changes in M.

Table 2: Thermo-physical properties of (H_2O) , (Cu)

Nanoparticles	ρ (kg/m ³)	C _p (J/kg K)	σ (S/m)	k (W/mK)	Pr
H ₂ O	997.1	4,179	0.05	0.613	6.2
TiO ₂	4,250	686.2	2.352 × 10 ⁻⁴	8.538	_

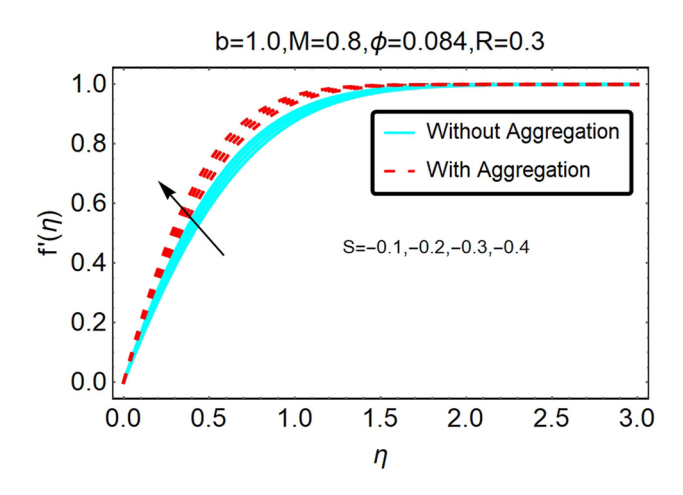


Figure 4: Velocity variation profile with changes in *S*.

Figure 4 illustrates the velocity profile changes as a measure of *S* drops. The velocity distribution typically rises as *S* value decreases. Even with aggregation, speeding up velocity is more effective than without it.

Figure 5 illustrates the velocity profile shifts as b changes. It is clear that as b rises, velocity falls until $\eta \approx 2$, at which point it rises for both the with and without aggregation cases. Even yet, aggregation still makes accelerating velocity more effective than aggregation alone.

5.3 Temperature profile for TiO₂-H₂O

Next, look at how the key parameters' temperature profiles behave. As this segment occurred, the temperature distribution was considered a deciding factor. These graphs can assess a flow's efficiency based on factors such as ϕ and R. The outcome is a rise in ϕ and R, which causes the temperature to rise next,

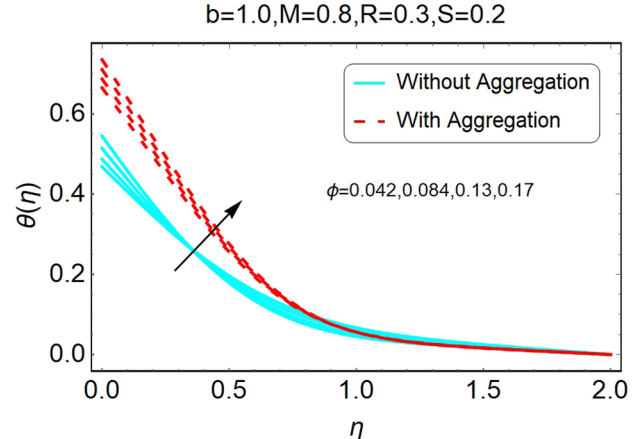


Figure 6: Temperature variation profile with changes in ϕ .

as shown in Figures 6 and 7. These graphs can assess a flow's performance based on several factors, including b, M, and S. Rising b, M, and S consequently lead to a drop in temperature, as shown in Figures 6–10.

The temperature curve as a result of ϕ value is depicted in Figure 6. ϕ increases, and the temperature increases as well. With aggregation, the temperature rises perform better than temperature rises without aggregation in terms of efficiency.

In the event of the decisive factor depicted in Figure 7, this section explores the temperature distribution over a range of *R* values. There is no doubt that the temperature will rise as *R* is increased. The effectiveness of temperature increase combined with aggregation is higher as the temperature rises alone.

According to the worth of b, as depicted in Figure 8, the temperature profile changes. When the turning factor occurs, such adjustments are visible in the temperature distribution. As expected, if the value of b is raised, the

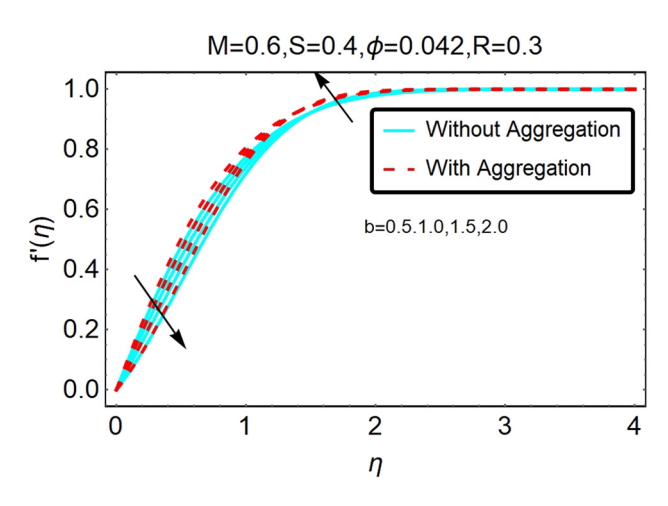


Figure 5: Velocity variation profile with changes in *b*.

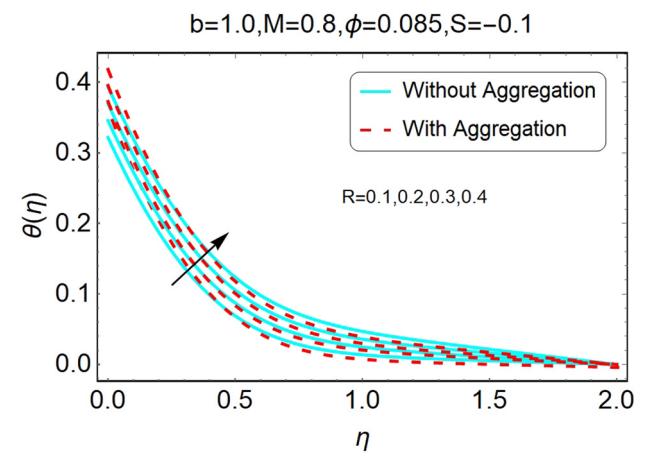


Figure 7: Temperature variation profile with changes in *R*.

8 — Basharat Ullah et al. DE GRUYTER

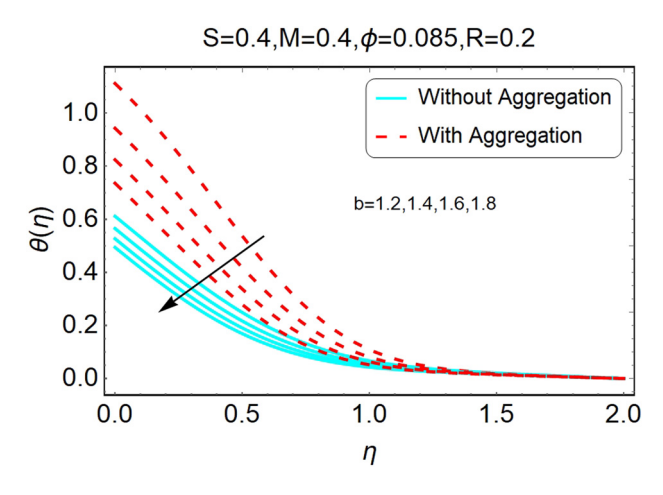


Figure 8: Temperature variation profile with changes in *b*.

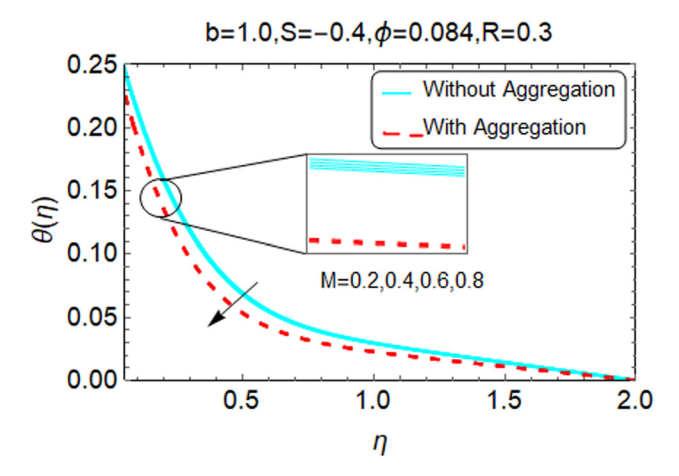


Figure 9: Temperature variation profile with changes in M.

temperature will fall. However, the efficiency of temperature reduction with aggregation is significant for temperature decrease without aggregation.

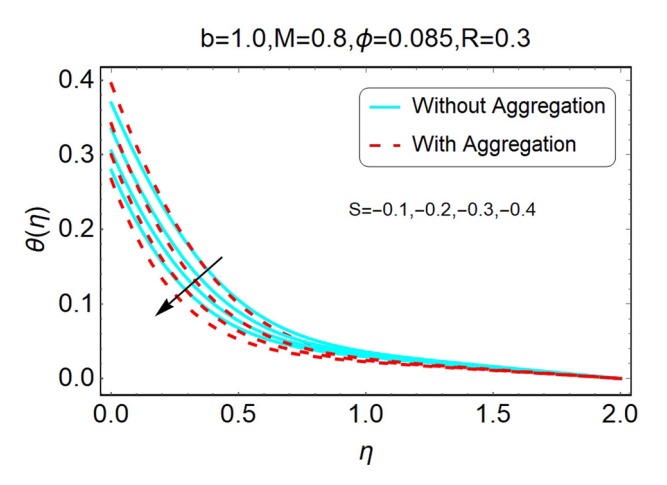


Figure 10: Temperature variation profile with changes in *S*.

The temperature profile $\theta(\eta)$ variations for different values of M are shown in Figure 9. Higher M values will result in a significant decrease in the temperature profile. However, the efficiency of decreasing temperature with aggregation is more vital than reducing without aggregation.

Throughout the range of temperatures in this section for the turning factor, for various values of S, the temperature profile variations are depicted in Figure 10. If we raise the value of S while lowering the temperature, it becomes apparent. However, the effectiveness of temperature reduction with aggregation is essential to reduce temperature without aggregation.

5.4 Comparison figures

Figures 11–13 illustrate a comparative analysis between two nanoparticles (aggregated particle and non-aggregated particle) and the findings obtained in the present study. The

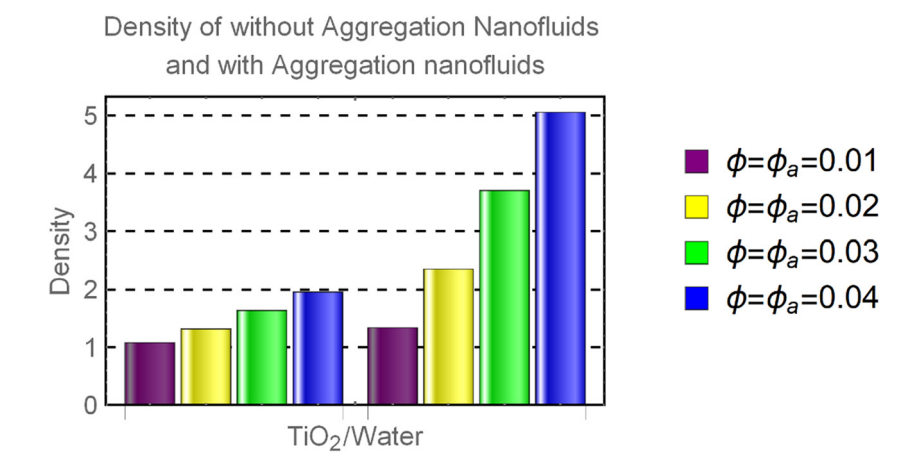


Figure 11: Variation of ϕ (without aggregation), $\phi_{\rm a}$ (with aggregation).

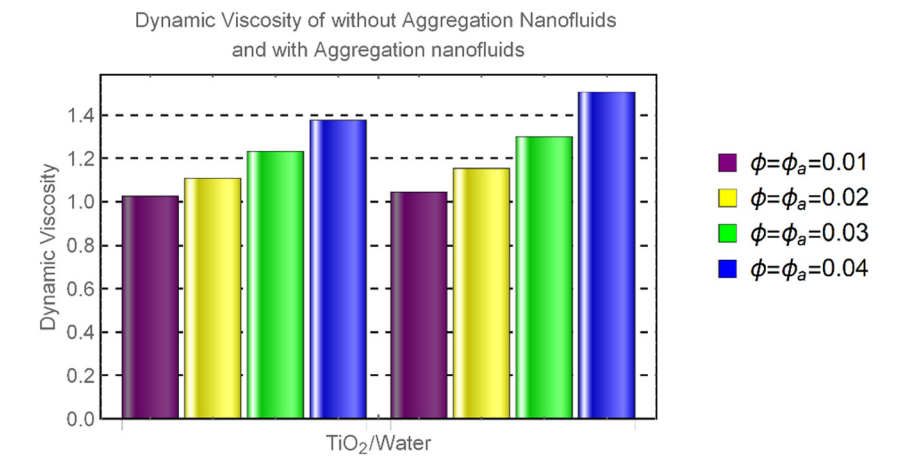


Figure 12: Variation of ϕ (without aggregation), $\phi_{\rm a}$ (with aggregation).

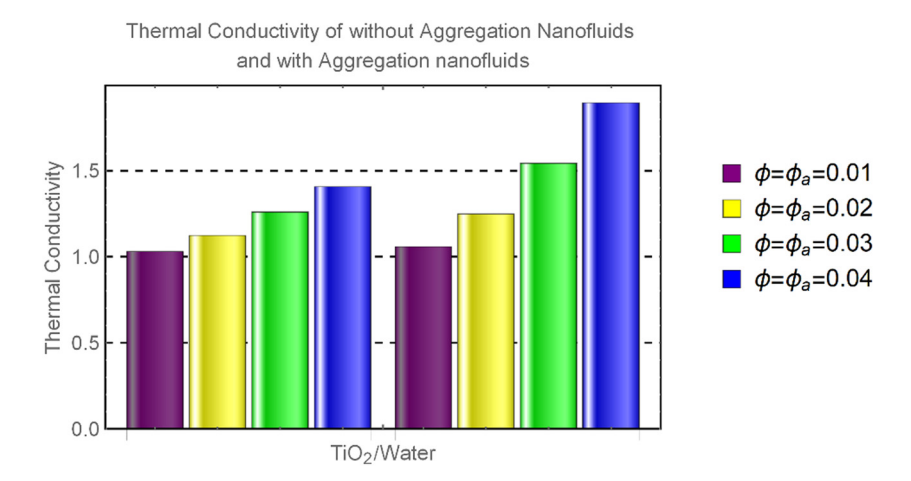


Figure 13: Variation of ϕ (without aggregation), ϕ_a (with aggregation).

present findings are consistent with prior research, indicating the dependability of the graphical scheme employed in this study and affirming the legitimacy of the results. Figures 11–13 illustrate a comparative investigation of the thermo-physical properties of both aggregated and non-aggregated nanoparticles of copper (TiO₂) and water. Figures 11–13 provide a clear demonstration that the density, dynamic viscosity, and thermal

conductivity of aggregated nanoparticles are significantly higher compared to non-aggregated nanoparticles. Nonetheless, water exhibits significantly low values for its physical properties. Figure 12 demonstrates that the density of aggregated nanoparticles is significantly higher compared to non-aggregated nanoparticles, which in turn exhibit a higher density than water. Figure 13 presents a comparative

Table 3: The code and model validation with the published data in the literature

Parameter		Khaled and Vafai [3]		Current study	
Squeezed flow	Magnetic parameter	Squeezed flow (a)	Magnetic parameter (<i>N</i>)	Squeezed flow (b)	Magnetic parameter (<i>M</i>)
0.5	2	3.46509	4.25791	3.46509	4.25791
1.0	4	3.46478	4.25791	3.46478	4.25751
1.5	6	3.46427	4.25791	3.46427	4.2571
2.0	8	3.2864	2.58156	3.2864	2.58156

examination of thermal conductivity, indicating that the thermal conductivity of aggregated nanoparticles is significantly higher in comparison to non-aggregated nanoparticles. The size and concentration of nanoparticles in the base fluid are significant elements that contribute to the enhanced performance of the aggregation nanofluid.

We use the comparison table with the previous work by A.R.A. Khaled and K. Vafai to evaluate the squeezed flow and magnetic parameter values in detail. Table data show that while squeezed flow parameter values are the same throughout both investigations, magnetic parameter values show minimal variation. The fact that the squeezed flow values at different points (0.5, 1.0, 1.5, and 2.0) are identical in both studies demonstrates a strong correlation in this regard. However, magnetic parameter values vary, possibly due to experimental conditions or methods. Compare the results to see that the squeezed flow is consistent and that the magnetic parameters differ slightly. This can lead to further investigation into the causes (Table 3).

6 Conclusions

Using a model with and without aggregation, we have examined how a nanofluid moves and transfers heat over a sensor under the influence of heat radiation surface in a two-dimensional laminar boundary layer. Once the parameter study is complete, we will comprehend the issue physically. In this study, a nanofluid is used, namely nanofluid $\text{TiO}_2/\text{H}_2\text{O}$. After figuring out the problem mathematically and graphically, we can draw the following conclusions:

- Based on the findings of the current study, it is suggested that aggregation nanoliquids have excellent heat transfer characteristics that would significantly improve the thermal process.
- When *M* is raised, the velocity distribution will grow.
- The velocity profile changes from 0 to 2 to 2 to 4 as *b* increases in value.
- The velocity distribution is affected in the same way by growing the value φ of as it is by raising it.
- When *S* is reduced, the speed distribution will expand.
- As the value of the parameter ϕ increases, so does the temperature profile.
- The temperature distribution well grows as the parameter *R* value climbs.
- The temporal pattern falls, increasing the parameter M' value.
- The shape of temperatures decreases as the parameter b value rises.

Acknowledgments: The study was funded by Researchers Supporting Project number (RSPD2024R749), King Saud University, Riyadh, Saudi Arabia.

Funding information: The study was funded by Researchers Supporting Project number (RSPD2024R749), King Saud University, Riyadh, Saudi Arabia.

Author contributions: All authors have accepted responsibility for the entire content of this manuscript and approved its submission.

Conflict of interest: The authors state no conflict of interest.

Data availability statement: The datasets generated and/ or analyzed during the current study are available from the corresponding author on reasonable request.

References

- Choi SU, Eastman JA. Enhancing thermal conductivity of fluids with nanoparticles (No. ANL/MSD/CP-84938; CONF-951135-29).
 Argonne, IL (United States): Argonne National Lab. (ANL); 1995.
- [2] Koo J, Kleinstreuer C. A new thermal conductivity model for nanofluids. J Nanopart Res. 2004;6:577–88.
- [3] Khaled AR, Vafai K. Hydromagnetic squeezed flow and heat transfer over a sensor surface. Int J Eng Sci. 2004;42(5–6):509–19.
- [4] Siddiqui AM, Irum S, Ansari AR. Unsteady squeezing flow of a viscous MHD fluid between parallel plates, a solution using the homotopy perturbation method. Math Model Anal. 2008;13(4):565–76.
- [5] Madhu M, Kishan N, Chamkha AJ. Unsteady flow of a Maxwell nanofluid over a stretching surface in the presence of magnetohydrodynamic and thermal radiation effects. Propul Power Res. 2017;6(1):31–40.
- [6] Sheikholeslami M, Vajravelu KJAM. Nanofluid flow and heat transfer in a cavity with variable magnetic field. Appl Math Comput. 2017;298:272–82.
- [7] Manjunatha S, Puneeth V, Gireesha BJ, Chamkha A. Theoretical study of convective heat transfer in ternary nanofluid flowing past a stretching sheet. J Appl Comput Mech. 2022;8(4):1279–86.
- [8] Abrar MN. Entropy analysis of double diffusion in a Darcy medium with tangent hyperbolic fluid and slip factors over a stretching sheet: Role of viscous dissipation. Numer Heat Transf Part A Appl. 2024;227:1–14.
- [9] Nadeem S, Abbas N, Malik MY. Inspection of hybrid-based nanofluid flow over a curved surface. Comput Methods Prog Biomed. 2020;189:105193.
- [10] Das S, Ali A, Jana RN. Darcy–Forchheimer flow of a magneto-radiated couple stress fluid over an inclined exponentially stretching surface with Ohmic dissipation. World J Eng. 2021;18(2):345–60.
- [11] Khan U, Adnan, Ullah B, Abdul Wahab H, Ullah I, Almuqrin MA, Khan I. Comparative thermal transport mechanism in $Cu-H_2O$ and

- Cu-Al₂O₃/H₂O nanofluids: numerical investigation. Waves Random Complex Media. 2022;28:1-16.
- [12] Khattak S, Ahmed M, Abrar MN, Uddin S, Sagheer M, Farooq Javeed M. Numerical simulation of Cattaneo-Christov heat flux model in a porous media past a stretching sheet. Waves Random Complex Media. 2022;36:1-20.
- Kumar B, Seth GS, Nandkeolyar R, Chamkha AJ. Outlining the impact of induced magnetic field and thermal radiation on magneto-convection flow of dissipative fluid. Int J Therm Sci. 2019;146:106101.
- [14] Das S, Ali A, Jana RN. Numerically framing the impact of magnetic field on nanofluid flow over a curved stretching surface with convective heating. World J Eng. 2021;18(6):938-47.
- [15] Khan U, Ullah B, Khan W, Adnan, Khan I, Fayz-Al-Asad M. Applied mathematical modelling and heat transport investigation in hybrid nanofluids under the impact of thermal radiation: numerical analysis. Math Probl Eng. 2021;2021(1):2180513.
- [16] Li X, Wen D, Guo Z. Investigation of nanoparticle aggregation and its effects on transport properties of nanofluids. J Nanopart Res. 2015;17:212.
- [17] Ellahi R, Hassan M, Zeeshan A. Aggregation effects on water base Al₂O₃ nanofluid over a permeable wedge in mixed convection. Asia-Pac J Chem Eng. 2016;11(2):179-86.
- [18] Gangadhar K, Bhargavi DN, Kannan T, Rao MVS, Chamkha AJ. Transverse MHD flow of Al₂O₃-Cu/H₂O hybrid nanofluid with active

- radiation: a novel hybrid model. Math Methods Appl Sci. 2020:43:8309-24.
- [19] Khaled AR, Vafai K. Heat transfer and hydromagnetic control of flow exit conditions inside oscillatory squeezed thin films. Numer Heat Transf Part A Appl. 2003;43(3):239-58.
- Chen J, Zhao CY, Wang BX. Effect of nanoparticle aggregation on the thermal radiation properties of nanofluids: an experimental and theoretical study. Int J Heat Mass Transf. 2020;154:119690.
- Reddy PS, Sreedevi K, Rao DN, Rao TS. Effect of nanoparticle [21] aggregation on thermal conductivity and viscosity of nanofluids: Experimental and theoretical studies. J Nanosci Nanotechnol. 2017;17(1):626-35.
- [22] Hussein AM, Bakar RA, Kadirgama K, Sharma KV. The effect of nanoparticles on laminar heat transfer in nanofluids: A review. Renew Sustain Energy Rev. 2013;29:734-43.
- [23] Krishna MV, Swarnalathamma BV, Chamkha AJ. Investigations of Soret, Joule and Hall effects on MHD rotating mixed convective flow past an infinite vertical porous plate. J Ocean Eng Sci. 2019;4(3):263-75.
- [24] Sarkar J, Bhattacharya R, Ajitkumar P. Nanofluid stabilized by nanoparticle aggregation for enhanced heat transfer performance. Int J Heat Mass Transf. 2018;126:712-23.
- [25] Rehman R, Khan U, Wahab HA, Ullah B. Second law analysis for the flow of hybrid nanofluid over a wedge. Waves Random Complex Media. 2022;32:1-16.